Longitudinal control of hybrid electric buses using traction motor and pneumatic braking system

JIE SHU, YONG ZHANG, CHENGLIANG YIN
Mechanical School, Shanghai Jiao Tong University
800 Dongchuan Road, Minhang District, Shanghai, CHINA
E-mail: qingdaoshu@gmail.com

Abstract- Additional energy source of hybrid electric buses comprises new control tasks. One of the main challenges of hybrid electric buses is the integrated control between traction motor and brakes, associated with which is the problem of switching traction motor and brakes. Existing control techniques only provide a result of frequent switch and jerky ride. In this paper, we propose a control strategy including two control laws, which are calculated simultaneously to optimize a certain tracking criterion by a fuzzy adaptive algorithm. Considering parametric uncertainties, the two control laws are used to determine whether to activate the traction motor or the pneumatic brake. The stability and convergence properties of the longitudinal brake control system are analytically proved by using Lyapunov stability theory and Barbalat's lemma. We examine the proposed algorithm with different mass uncertainties and the simulation results demonstrate stable behaviors when two buses drive into a bus station.

Keywords- hybrid electric bus; platoon performance; coordinated control; fuzzy adaptive control; sliding mode control

1 Introduction

With rising public concern about fuel economy and emission requirements in automobiles, interest in hybrid electric vehicles has never been greater. In the present hybrid power train systems, the brake action of a vehicle is generally achieved by hydraulic/pneumatic brake system and regenerative braking system [1, 2]. When hybrid electric vehicles, such as series-parallel hybrid electric buses, are driving with a stop-and-go pattern in urban areas, effective regenerative braking can significantly improve the fuel economy. However, the regenerative braking directly affects modelling and control design, which adds some complexity to the brake control design. It's recognized that longitudinal control problems in hybrid electric vehicles are quite different from those encountered in the control design for general vehicles [3, 4]. The capacity of regenerative braking changes with varying factors, such as the battery SOC (state-of-charge), vehicle speed and brake pedal position [5]. Therefore, the design of integrated control between traction motor and brake is an important subject in the longitudinal control of hybrid electric buses.

During recent years, different cruise control strategies have been proposed to the problem of vehicle safety and passenger comfort [6-8]. While the problem of cruise control has been deeply explored by researchers; some work still needs to be done for the longitudinal control system of the hybrid electric buses with the capability of autonomously stopping at bus stations on the road, while keeping good passenger comfort and safety. The main current brake controls of hybrid electric vehicles are focused on regenerative braking with minimized stopping distance, regenerative braking with optimal energy recovery, and the cooperation between the hydraulic/pneumatic braking system and the regenerative braking system. In [9], a control strategy of motor regenerative braking for a mild hybrid vehicle is established, where the disturbance of road conditions and the nonlinear characteristic of hydraulic dynamic processes are not considered. [10] introduces a new anti-skid re-adhesion control considering the air brake, which carries out the cooperation control of regenerative braking and pneumatic brake system. In [11], a computational procedure to maximize the regenerated brake energy during braking is presented and the relationship between the regenerated brake energy and the power train components is surveyed.

As for the longitudinal braking control for heavy duty vehicles, such as a city bus, the large mass of a hybrid electric bus demands large braking force during deceleration and the regenerative braking torque cannot be made as much as possible to provide all the required braking torque. The model mismatch, measurement noise, actuator time delay and external disturbances can affect the brake control system design. The sliding mode control techniques and fuzzy control have been applied to longitudinal braking control, but the accurate motion control is yet to be achieved. To remedy this problem, various control approaches are applied to adjust the actuator pressure to force the vehicle to stop in a desired manner [12, 13]. Generally, the control objective of these control method is to make the vehicle track a desired velocity or to follow the preceding vehicle within the safety distance. Vehicles equipped with advanced brake systems that can make the drivers feel more comfortable would dominate the markets, therefore smooth braking trajectory control would be an inevitable trend in the future automotive engineering [14].

In this paper a sliding mode controller incorporating the fuzzy adaptive concept will be developed to control a hybrid electric bus to stop at a bus station by following a preceding bus. In section 2, the mathematical model of the series-parallel hybrid electric bus is introduced. Section 3 is devoted to the development of the control strategy, where a stable adaptive fuzzy inference system is embedded in boundary layer to cope with the uncertainties and disturbances that would arise during the braking process. Some simulation experimental results are presented in Section 4 and some final comments and further research directions are gathered in Section 5.

2 Model Formulation

2.1 Powertrain configuration

In the powertrain model of the hybrid electric bus [15], seen in Figure 1, there are three different sources of torque, namely, ICE, integrated starter-generator (ISG) and traction motor (TM) in the series-parallel powertrain configuration. They work together with clutch and transmission to form different driving modes. Moreover, the high-voltage battery is the energy storage device for the bus. A separate controller, called energy management system (EMS), is used to coordinate the energy distribution among those controllers of ICE, ISG, TM and high-voltage battery. The regenerative braking is achieved by the TM and its brake torque can be sent by the EMS via CAN (Control Area Network) bus system.

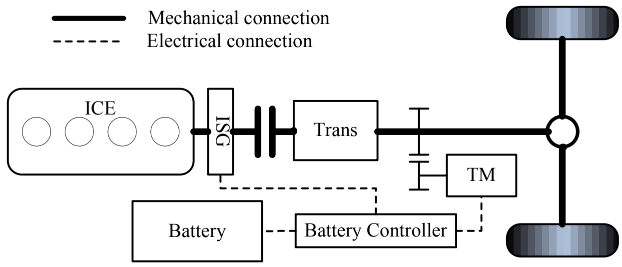

Figure 1 Configuration of series-parallel powertrain for a hybrid electric bus

2.2 Vehicle Model

The dynamic equation for a vehicle model is obtained for a straight-line braking event. An *F=ma* force balance for the vehicle is described by the following equation:

$$M\frac{dv}{dt} = F_{xf} + F_{xr} - F_d \tag{1}$$

where

M Vehicle mass including wheels;
v Vehicle longitudinal velocity;
F_{xf} Road force on the front wheels;
F_{xr} Road force on the rear wheels;
F_d Drag forces due to wind and grade.

2.3 Wheel model

With moment balances, the dynamic equations for the driving wheels (rear wheels) and the driven wheels (front wheels) are:

$$\begin{cases} J_{wf}\dot{\omega}_{wf} = -rF_{xf} - M_f - T_{bf} \\ J_r\dot{\omega}_r = T_e + T_{TM} - rF_{xr} - M_r - T_{br} \end{cases} \tag{2}$$

where

J_{wf}, J_r Inertia of front wheels and axle;
$\dot{\omega}_{wf}, \dot{\omega}_r$ Angular acceleration of wheels;
F_{xf}, F_{xr} Road forces on wheels;
M_f, M_r Rolling resistance of wheels;
T_{bf}, T_{br} Brake torques on wheels;
T_{TM} Driving torque from the traction motor;
T_e Axle shaft torque;
r Wheel radius.

2.4 Longitudinal Dynamics Model

At low levels of deceleration, wheel slip is quite small for an ordinary vehicle [16]. It's fundamentally the same for a bus driving into a bus station at low speed, in that the pneumatic brake and regenerative brake are used to generate moderate longitudinal resistance effort. For a smooth stopping, the bus braking is usually kept smooth to ensure the passenger comfort. Therefore, the wheel slip λ can be assumed to be negligible, then the kinematic rolling condition has $\dot{\omega}_{wf} = \dot{\omega}_r = \dot{v}/r$, and the dynamic equations of (1) and (2) are solved as:

$$\begin{aligned}&[T_e + T_{TM} - T_{bf} - T_{br} - M_r - M_f]/r - F_d \\ &= (m + (J_r + J_{wf})/r^2)a\end{aligned} \tag{3}$$

Let T_b be the total pneumatic brake torque and M_{lr} be the lumped rolling resistance, and substitute $J_r = J_{wr} + J_e$ for the lumped rear wheels/powertrain inertia, (3) can be rewritten as follows:

$$\begin{aligned}&T_e + T_{TM} - T_b - M_{lr} - F_d r \\ &= (J_e + (mr^2 + J_{wr} + J_{wf})R_{dr}^2)a/r/R_{dr}^2\end{aligned} \tag{4}$$

where R_{dr} is the ratio of the wheel rotational speed to the engine rotational speed, $M_{lr} = C_r \cdot m \cdot g \cdot r$ and $F_d = C_a \cdot v^2$. By defining

$$M_L = \frac{1}{rR_{dr}^2}(J_e + R_{dr}^2(mr^2 + J_{wr} + J_{wf})) \tag{5}$$

Assume that the traction motor input doesn't have time delays and the time delays of the pneumatic system is τ_p, and we obtain

$$T_e(t) + T_{TM}(t) - T_b(t - \tau_p) - M_{lr} - F_d r = M_L \cdot a(t) \tag{6}$$

In the particular case of stopping a hybrid electric bus at a bus station, the torque from ICE described in Figure 1 is cut off by the clutch. Let x_1 be the longitudinal displacement and x_2 be the vehicle speed during the longitudinal motion. Considering the disturbance d caused by road conditions, (6) can be described as:

$$\begin{cases}\dot{x}_1 = x_2 \\ M_L \cdot \dot{x}_2 + M_{lr} + C_a \cdot r \cdot x_2^{\,2} + d = u\end{cases} \tag{7}$$

where u is the composite input torque of engine, traction motor and pneumatic brake. However, according to the EMS strategy, the engine is usually shut off when a hybrid electric vehicle is driving at a low speed. So in the following sections, u is only the composite input torque of traction motor and pneumatic brake. With respect to the uncertainties of the longitudinal dynamic model, the following physically motivated assumptions can be made:

Assumption 1. The parameter M_L is time varying and unknown due to the varying number of passengers, but it is positive and bounded, i.e. $0 < M_{L\_\min} < M_L < M_{L\_\max}$.

Assumption 2. The parameter C_a is unknown but positive and bounded, i.e. $0 < C_{a\_\min} < C_a < C_{a\_\max}$.

Assumption 3. The parameter C_r is known and constant. The disturbance caused by variations of road is included in d, which is unknown but bounded, i.e. $|d| < \delta$.

2.5 Brake model

The pneumatic brake system is the most prevalent in heavy-duty buses for public transportation. When a driver presses the brake pedal, the brake valve is opened and compressed air flows from air tank to the brake chambers. The brake chamber is a diaphragm actuator which converts the energy of air pressure to mechanical force. A nonlinear dynamic model has been developed for a valve-controlled brake chamber and a pneumatic brake system. The dynamic behaviour is modelled as a pure time delay followed by a brief linear second-order system [13].

$$\begin{cases}\dot{z}_1 = z_2 \\ \dot{z}_2 = -a_1 z_1 - a_2 z_2 + b_1 u_f \\ P_{whl} = z_1\end{cases} \tag{8}$$

Where

u_f Input to the treadle (foot) valve;

P_{whl} Brake pressure at the wheel.

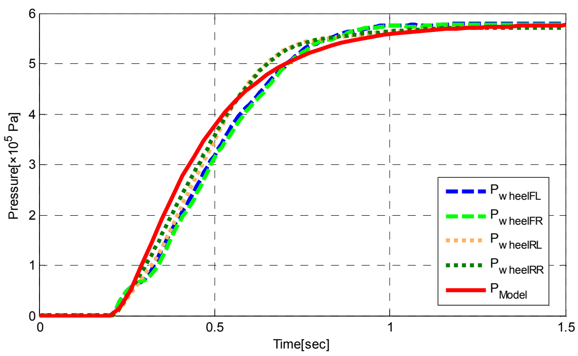

Figure 2 Comparison of actual brake and nonlinear model responses for step input

In order to validate the dynamic model and determine model parameters in (8), four brake pressure measurements from brake pressure transducers located in 4 different positions are presented in Figure 2. These 4 pressures are measured when the initial speed of the hybrid bus is 60km/h and a step input is applied to the brake pedal. The time response of the brake pressure model shown in equation (8) is plotted together in Figure 2 to show the accuracy of the proposed model.

During the stopping at a station, the bus braking is usually kept smooth to ensure passenger comfort and the longitudinal slip λ is generally small during this braking process. Therefore, the brake torque T_b is assumed to be proportional to the pressure difference between the applying brake pressure at the wheel and push-out pressure $P_o = 34.5\text{kPa}$.

$$T_b = \begin{cases} K_b(P_{whl} - P_o), \text{if } P_{whl} > P_o \\ 0 \qquad , \text{otherwise} \end{cases} \tag{9}$$

Where K_b is the brake torque coefficient or called 'brake torque gain'. This assumption is reasonable when the brake pressure is sufficiently large. Under this condition, the preload on the brake chamber return spring is omitted when brake torque is applied.

2.6 Deceleration and Jerk Profiles

The brake system can prevent the bus-to-bus space from dropping to an unsafe level when several buses enter a bus station in a fleet. It was reported that vehicle decelerations up to 2.5m/s^2 were comfortable to human passengers [17]. According to the research from simulator tests, the presence of steps in the jerk profile, which is the time rate of deceleration change, also has a significant effect on ride comfort [13]. From experimental tests, the magnitude of the jerk should not exceed 10 m/s^3 for passengers' safety. Apart from the peak value of the deceleration, the shape of the deceleration profile is important considering the passenger comfort. In Figure 5, the deceleration profile has been designed to serve as a reference for brake in this research.

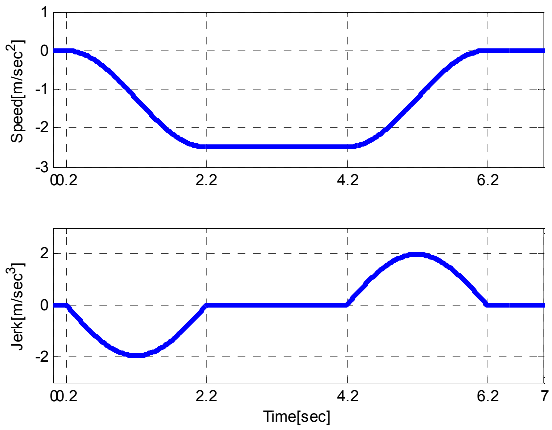

Figure 3 Deceleration profile for the brake control

3 Adaptive fuzzy Controller Design

3.1 Certainty Equivalence Control Term

The basic control task of controlling a hybrid electric bus to stop at a bus station is to control the bus to track the preceding bus at a safe distance. Figure 3 illustrates the definitions of spacing errors for the following bus.

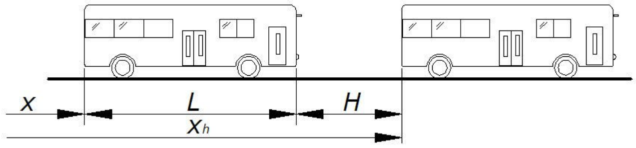

Figure 4 Safety spacing between two buses

Let the spacing error of the deceleration profile be:

$$e(t) = (x_1(t) + H) - x_h(t) \tag{10}$$

Let

$$\Lambda = [\lambda_0, \lambda_1, \cdots, \lambda_{rd-2}, 1]^{\mathrm{T}} \tag{11}$$

be a vector of design parameters and

$$e_s(t) = e^{(rd-1)}(t) + \lambda_{d\text{-}2} e^{(rd-2)}(t) + \cdots + \lambda_1 \dot{e}(t) + \lambda_0 e(t) \tag{12}$$

where rd is the relative degree of the dynamic system. Let

$$L(s) = s^{rd-1} + \lambda_{rd-2} s^{rd-2} + \cdots + \lambda_1 s + \lambda_0 \tag{13}$$

and assume that the design parameters in (11) are chosen so that $L(s)$ has its roots in the left half plane. Notice that $e_s(t)$ is a measurement of the tracking error. Considering model (7) where rd =2 so $\Lambda = [\lambda_0, 1]^{\mathrm{T}}$ and

$$e_s(t) = \dot{e}(t) + \lambda_0 e(t) \tag{14}$$

For $L(s)$ to have its roots in the left half plane, λ_0 is selected to be a strictly positive constant.

Regarding the development of the control law, the following assumptions are made:

Assumption 4. The states x_1 and x_2 are available.

Assumption 5. The velocity $\dot{x}_h$ and acceleration profile $\ddot{x}_h$ of the preceding bus desired trajectory are available and bounded.

Then the certainty equivalence control term is defined as

$$u_{ce} = \hat{M}_L \cdot (\ddot{x}_h - \lambda_0 \dot{e}(t)) + M_{lr} + \hat{C}_a \cdot r \cdot x_2^{\ 2} + \hat{d} \tag{15}$$

where $\hat{M}_L$, $\hat{C}_a$, $\hat{d}$ are estimates of M_L , C_a , d respectively.

3.2 Sliding Mode Control Term

We define the sliding mode control term as $u_{si} = -\eta \cdot \text{sgn}(e_s)$, where η is the control gain and

$$\text{sgn}(e_s) = \begin{cases} 1 & \text{if } e_s > 0 \\ 0 & \text{if } e_s = 0 \\ -1 & \text{if } e_s < 0 \end{cases} \tag{16}$$

Considering the Assumptions 1 and 2, it can be easily seen that $\left|\hat{C}_a - C_a\right| \le \left|C_{a\_\max} - C_{a\_\min}\right| = \varsigma$ and

$M_{L\_\min} / M_{L\_\max} \le \hat{M}_L / M_L \le M_{L\_\max} / M_{L\_\min} = \tau_M$. With η being properly chosen, the sliding condition

$$u_{si} = -\eta \cdot \mathrm{sgn}(e_s) \tag{17}$$

can be sufficiently imposed by:

$$u = u_{ce} + u_{si} \tag{18}$$

Where

$$u = \begin{cases} u_1(t), & \text{if } u_{ce}(t) + u_{si}(t) > 0, \\ 0, & \text{if } u_{ce}(t) + u_{si}(t) < 0 \text{ and } t_s \le t \le t_s + \tau, \\ u_2(t-\tau), & \text{if } u_{ce}(t) + u_{si}(t) < 0 \text{ and } t \ge t_s + \tau \end{cases} \tag{19}$$

Here t_s is the starting time of switching, $u_1(t)$ represents the traction motor control, $u_2(t-\tau)$ represents the pneumatic brake control and τ is the pure time delay of the pneumatic brake system.

3.3 Parameter Adaptation Law

In order to obtain an approximation to the disturbance $d(t)$, the estimate $\hat{d}(t)$ will be computed by fuzzy adaptive algorithm. The basic configuration of a fuzzy logic system consists of a fuzzifier, some fuzzy If-Then rules, a fuzzy inference engine and a defuzzifier. The full fuzzy adaptive controller has been presented in my another paper [18] and in this paper we only give the result.

Considering the system (7) with the feedback controller (18), let the adaptation law of the adjustable parameter vector be

$$\dot{\hat{\theta}} = -\varphi \cdot e_s \cdot \Psi(e_s) \tag{20}$$

where φ is a strictly positive constant and determines the convergence rate of $\hat{\theta}$. The chosen adaptation law can both provide a good approximation to disturbance and assure the convergence of the state variables for the purpose of profile tracking.

Theorem 1. Consider the longitudinal dynamic system represented by (7) . Then, for any conditions that subject to Assumptions 1-5, the controller (18) can ensure the asymptotic tracking and the convergence of the states.

Proof. See the proof in another paper [18].

The feedback controller is developed on the Assumption 1. However, the mass of a series-parallel hybrid electric bus can vary largely from a passenger carrying ability of no payload to full payload. Therefore, a longitudinal controller that is tuned for a range of mass, might be too aggressive or too slow for a different mass. So we need to estimate the mass of the bus and make sure that the Assumption 1 can be satisfied.

Consider the longitudinal dynamic system represented by (7). Let $\hat{M}_L$ denote the estimates of M_L and $\tilde{M}_L$ represent the estimation error ($\tilde{M}_L = \hat{M}_L - M_L$). A simple discontinuous projection $\mathrm{Proj}_{\hat{M}_L}$ can be defined [19, 20] as

$$\mathrm{Proj}_{\hat{M}_L}(\bullet) = \begin{cases} 0, & \text{if } \hat{M}_L = M_{L\_\max} \text{ and } \bullet > 0 \\ 0, & \text{if } \hat{M}_L = M_{L\_\min} \text{ and } \bullet < 0 \\ \bullet, & \text{otherwise} \end{cases} \tag{21}$$

Suppose that the parameter estimates $\hat{M}_L$ is updated by the following projection type adaptation law,

$$\dot{\hat{M}}_L = \mathrm{Proj}_{\hat{M}_L}(\Gamma \cdot \tau_{M_L}), \ \hat{M}_L(0) \in \Omega_{M_L} \tag{22}$$

where $\Gamma(t) > 0$ is any continuously differentiable positive symmetric adaption rate matrix and τ_{M_L} is an adaptation function to be synthesized later. And Γ is updated by,

$$\dot{\Gamma} = \alpha_{M_L}\Gamma - \frac{\Gamma\Omega\Omega^T\Gamma}{1 + v\Omega^T\Gamma\Omega} \tag{23}$$

where $\alpha_{M_L} \ge 0$ is the forgetting factor and v is used to ensure the adaptation function to have the un-normalized form. With this adaptation law, the following desirable properties hold:

$$\begin{aligned} &\text{P1.} \quad \hat{M}_L \in \Omega_{M_L} \triangleq \{M_L : M_{L\_\min} < M_L < M_{L\_\max}\} \\ &\text{P2.} \quad \tilde{M}_L^{\mathrm{T}}(\Gamma^{-1} \cdot \mathrm{Proj}_{\hat{\theta}}(\Gamma \cdot \tau_{M_L}) - \tau_{M_L}) \le 0, \ \forall \tau_{M_L} \end{aligned} \tag{24}$$

4 Simulation Results

The simulation studies are performed to show the effectiveness of the proposed adaptive fuzzy control scheme, considering a situation in which two buses are driving into a bus station in a line. Both wheel velocity and vehicle velocity of the controlled bus are assumed available. For the fuzzy system, triangular and trapezoidal membership functions are adopted for the parameter adaptation law, with the central values being defined as c=[-15 -3 -0.35 0 0.35 3 15]*0.95*10^(-2). The initial values for the vector of adjustable parameters are $\hat{\theta} = 0$, and are updated at each iteration step according to the adaptation law of (20). Considering the deceleration profile and jerk profile in Section 2.6, the displacement trajectory and velocity trajectory in Figure 5 and Figure 6 are selected for the preceding bus. The initial velocity of bus, as the controller brake torque is applied, is set to be 30km/h. The simulations are done in 2 different cases for braking with 0.05s actuator delays:

$\Delta M = 50$ and $\Delta M = 200, \Delta C_a = 0.5$. The obtained results are presented from Figure 7 to Figure 11.

During the simulations, the following values are chosen: $M_L = 6200\text{kg}$, $C_a = 1.5$, $C_r = 0.01$, $\varphi = 3000$, $\lambda_0 = 0.2$. In order to test the robustness feature of the proposed control schemes, both the external disturbance and model parameter uncertainties are considered. The actual parameters of the bus are assumed to be different from their normal values, i.e. $\hat{M}_L = 6250/6400\text{kg}$, $\hat{C}_a = 2.0$.

Figure 7 shows the estimates of the external disturbance. The solid line and dash dot line represent the numerical simulation result of our proposed control scheme and the dash line represents the predefined disturbance into the controlled bus. At time t=0s, there is a large error between the estimated disturbance and its real value. This is caused by the brake delay at the beginning. However, the estimate approximates its real value gradually after 1 second with the adjustment of the fuzzy adaptive law. The large fluctuation of the estimate happens at t=1.8s, when the preceding bus meets a disturbance in longitudinal velocity. The larger the mass uncertainty is, the larger the estimate error amplitude is. We can see that the mass uncertainty does affect the estimate amplitude, but the estimate can converge to its real value in both cases after a short time of adjustment. Moreover, if there is a mass uncertainty happens, then the estimate can also reflect the change shown in the difference between the solid line and dash dot line, which is different in 2 cases. So the proposed fuzzy adaptive algorithm can be used to estimate the external disturbance.

The control input of the system can be seen in Figure 8. The solid line and dash dot line represent the results with parameter uncertainties and actuator delay in consideration, while the dash line is the result without considering parameter uncertainties and actuator delay. The brake delay of both cases can be well illustrated at t=0s, where a brake delay about 0.05s can be easily seen. Note that the brake delay in $\Delta M = 50$ is less than that in $\Delta M = 200, \Delta C_a = 0.5$, which may be resulted from the adjustment for different mass of the fuzzy adaptive algorithm in those 2 cases. Usually, the larger the parameter uncertainties are, the longer the brake delay is. According to control law(19), we can see in both cases that the drive mode keeps brake control in 0.05 after getting the switch signal, and then it begins traction motor control.

Figure 9 and 10 show the simulation results of spacing and velocity tracking errors. Small spacing error and good velocity tracking error are achieved. However, we can see that larger mass uncertainty leads to larger tracking error but the controller can still make the error converge at a constant around reference inputs. Notice that the spacing error and velocity error of the second case appear to be larger in contrast with those in the first case. However, the performance of the controlled bus is still good for achieving the spacing and switching process. We can see small jerk for both cases in Figure 11 compared with that of original control.

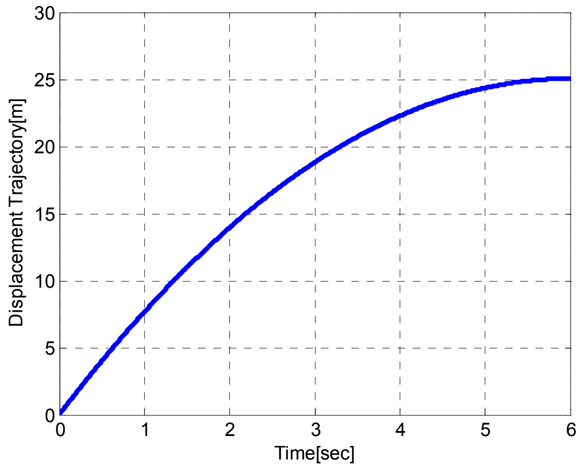

Figure 5 Displacement trajectory for the preceding bus

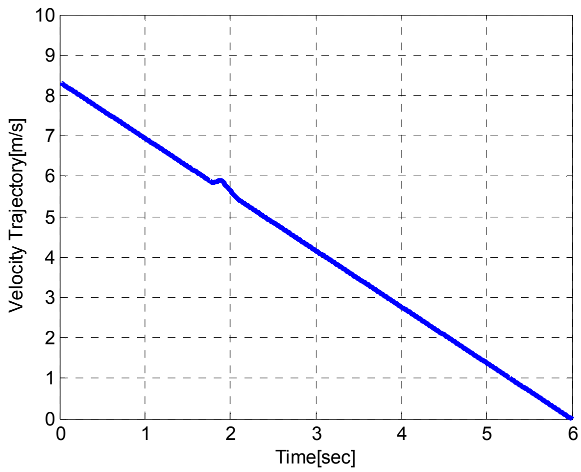

Figure 6 Velocity trajectory for the preceding bus

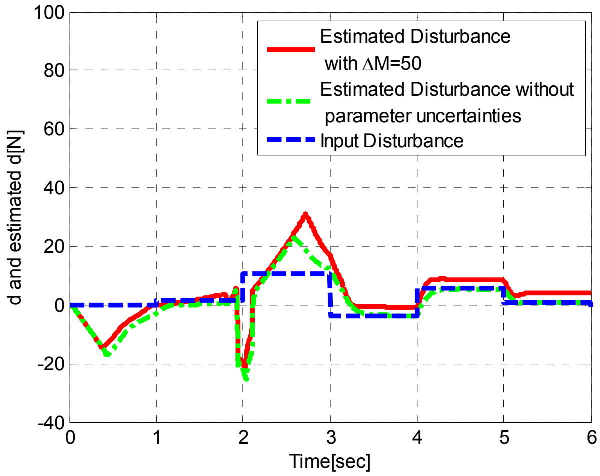

(a) Brake with $\Delta M = 50$ and 0.05s delays

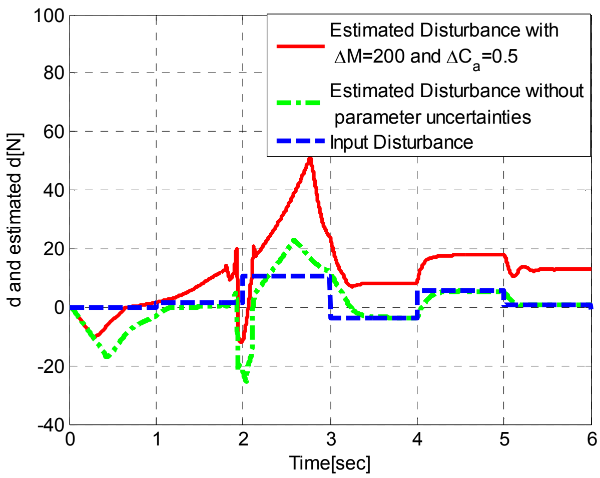

(b) Brake with $\Delta M = 200, \Delta C_a = 0.5$ and 0.05s delays

Figure 7 Disturbance d and its estimate $\hat{d}$

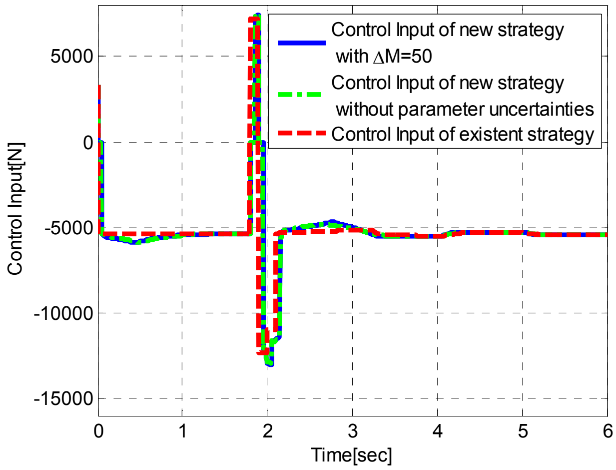

(a) Brake with $\Delta M = 50$ and 0.05s delays

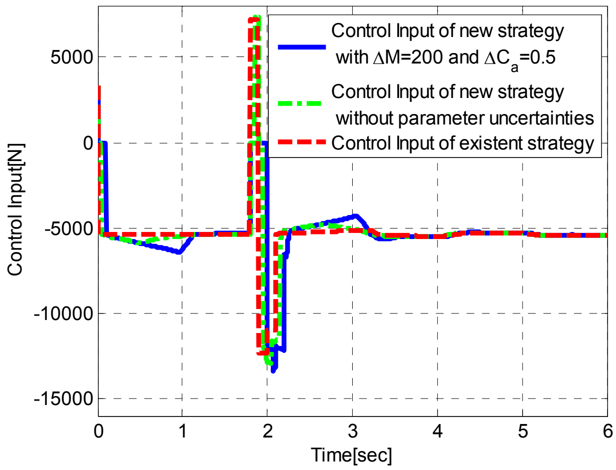

(b) Brake with $\Delta M = 200, \Delta C_a = 0.5$ and 0.05s delays

Figure 8 Control input u

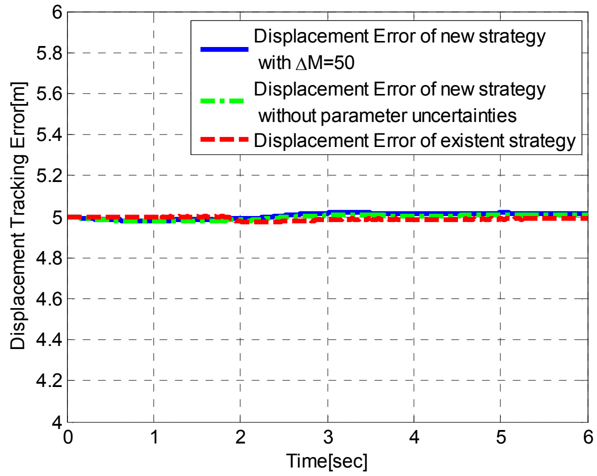

(a) Brake with $\Delta M = 50$ and 0.05s delays

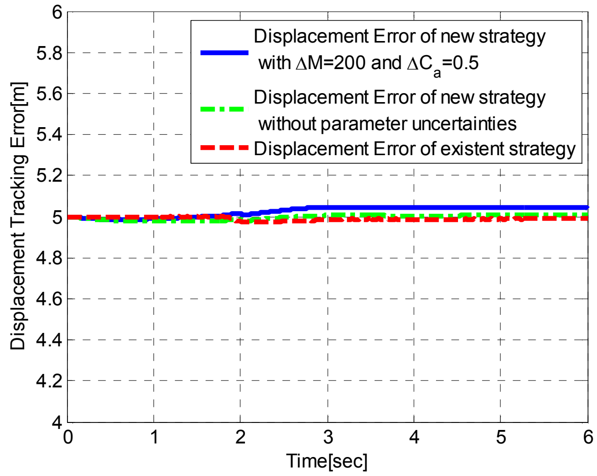

(b) Brake with $\Delta M = 200, \Delta C_a = 0.5$ and 0.05s delays

Figure 9 Spacing between controlled bus and preceding bus

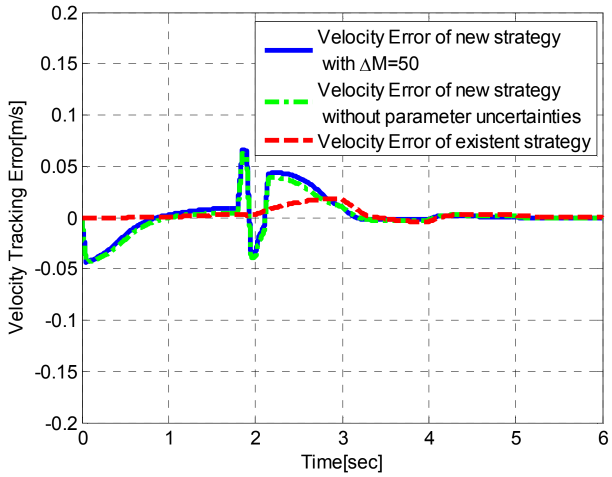

(a) Brake with $\Delta M = 50$ and 0.05s delays

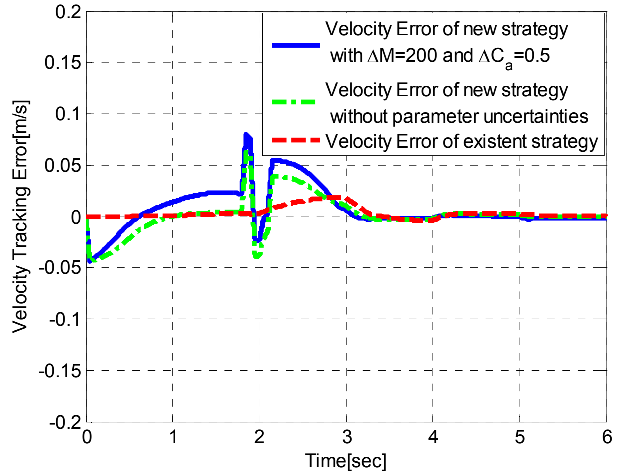

(b) Brake with $\Delta M = 200, \Delta C_a = 0.5$ and 0.05s delays

Figure 10 Velocity tracking error between controlled bus and preceding bus

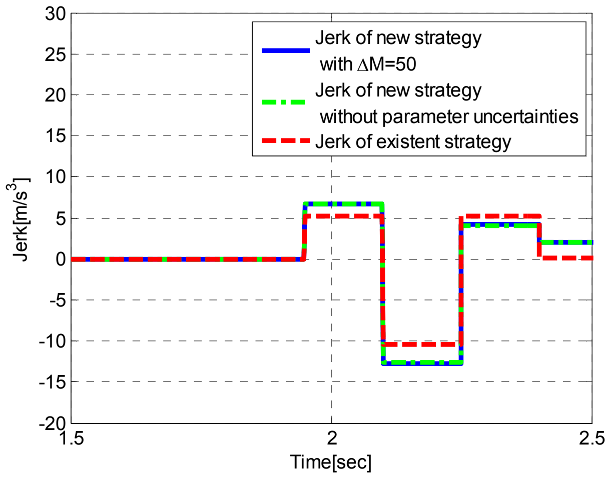

(a) Brake with $\Delta M = 50$ and 0.05 delays

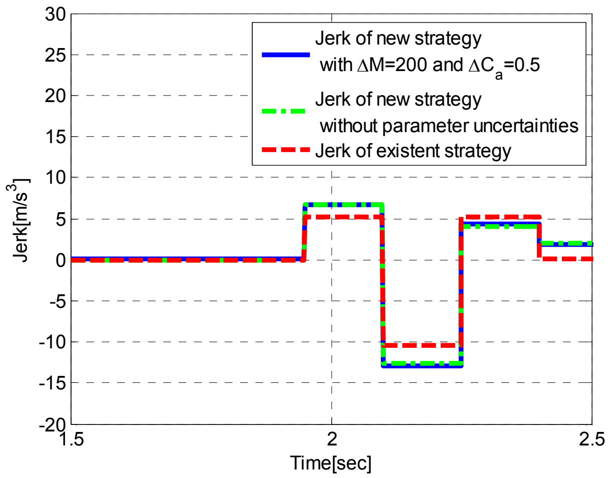

(b) Brake with $\Delta M = 200, \Delta C_a = 0.5$ and 0.05s delays

Figure 11 Jerk of the switching point

5 Conclusions

The present paper explores the possibility of coordinating the control between traction motor and pneumatic brake for a series-parallel hybrid electric bus to follow a preceding bus to stop at a bus station. To enhance the tracking performance, the adopted scheme is embedded with an adaptive fuzzy algorithm for compensating the dynamic model uncertainty and external disturbance. The state switch strategy presented in this paper makes the bus operate in 3 possible modes during a brake process: traction motor control, pneumatic brake control and zero control. The control objective is to maintain the safety distance from the preceding bus while keeping passenger comfort. The stability and convergence properties of the closed-loop systems are analytically proved by using Lyapunov stability theory and Barbalat's lemma. The simulation results demonstrate that the proposed controller has an improved performance over the original controller. To further investigate the potentialities and the limits of our proposed control scheme, there is an obvious need of prototype validation or experiments on small-scale hybrid electric buses, which is the future direction of the present research.

Acknowledgement

This research has been partially supported by *The research and development of SWB6116 hybrid electric bus* (Grant No. 2006AA11A127, The National High Technology Research and Development Program of China) and partially supported by the Shanghai Postdoctoral Sustentation Fund, China (Grant No. 07R214205) .

References:

[1] S. R. Cikanek and K. E. Bailey, Regenerative braking system for a hybrid electric vehicle, *Proceedings of the American Control Conference*, Anchorage, AK, 2002, pp. 3129-3134.

[2] L. W. Tsai, G. Schultz, and N. Higuchi, A novel parallel hybrid transmission, *Journal of Mechanical Design, Transactions of the ASME*, Vol. 123, pp. 161-168, 2001.

[3] S. Drakunov, U. Ozguner, P. Dix, and B. Ashrafi, ABS control using optimum search via sliding modes, *IEEE Transactions on Control Systems Technology*, Vol. 3, pp. 79-85, 1995.

[4] C. M. Lin and C. F. Hsu, Self-learning fuzzy sliding-mode control for antilock braking systems, *IEEE Transactions on Control Systems Technology*, Vol. 11, pp. 273-278, 2003.

[5] C. C. Lin, H. Peng, J. W. Grizzle, and J. M. Kang, Power management strategy for a parallel hybrid electric truck, *IEEE Transactions on Control Systems Technology*, Vol. 11, pp. 839-849, 2003.

[6] A. Ferrara and C. Vecchio, Second order sliding mode control of vehicles with distributed collision avoidance capabilities, *Mechatronics*, Vol. 19, pp. 471-477, 2009.

[7] D. Swaroop, J. K. Hedrick, and S. B. Choi, Direct adaptive longitudinal control of vehicle platoons, *IEEE Transactions on Vehicular Technology*, Vol. 50, pp. 150-161, 2001.

[8] A. Ferrara and C. Vecchio, Collision avoidance strategies and coordinated control of passenger vehicles, *Nonlinear Dynamics*, Vol. 49, pp. 475-492, 2007.

[9] D. Qin, M. Ye, and Z. Liu, Regenerative braking control strategy in mild hybrid electric vehicles equipped with automatic manual transmission, *Frontiers of Mechanical Engineering in China*, Vol. 2, pp. 364-369, 2007.

[10] S. Kadowaki, K. Ohishi, S. Yasukawa, and T. Sano, Anti-skid re-adhesion control based on disturbance observer considering air brake for electric commuter train, *International Workshop on Advanced Motion Control, AMC*, Kawasaki, 2004, pp. 607-612.

[11] J. Hellgren and E. Jonasson, Maximisation of brake energy regeneration in a hybrid electric parallel car, *International Journal of Electric and Hybrid Vehicles*, Vol. 1, pp. 95-121, 2007.

[12] M. Amodeo, A. Ferrara, R. Terzaghi, and C. Vecchio, Slip control for vehicles platooning via second order sliding modes, *IEEE Intelligent Vehicles Symposium, Proceedings*, Istanbul, 2007, pp. 761-766.

[13] K. Yi and J. Chung, Nonlinear brake control for vehicle CW/CA systems, *IEEE/ASME transactions on mechatronics*, Vol. 6, pp. 17-25, 2001.

[14] J. H. Yang and C. C. Yang, Adaptive sliding mode control for vehicle brake systems with fuzzy composition, *International Journal of Modelling, Identification and Control*, Vol. 4, pp. 112-126, 2008.

[15] J. Shu, W. Xiong, C. Yin, and Y. Zhang, Effective regenerative braking control for smooth stop of a hybrid electric bus, *2008 IEEE Vehicle Power and Propulsion Conference, VPPC 2008*, Harbin, 2008.

[16] F. Gustafsson, Slip-based tire-road friction estimation, *Automatica*, Vol. 33, pp. 1087-1098, 1997.

[17] P. Seiler, C. Shaw, and B. Song, Application of nonlinear control to a collision avoidance system, *Proceedings of the 5th World Congress on Intelligent Transport Systems*, Seoul, 1998.

[18] J. Shu, L. Chen, J. Yao, and C. L. Yin, Application of switching traction and braking systems in longitudinal control for series-parallel hybrid electric buses, International Journal of Vehicle Design, Submitted, 2009.

[19] S. Boyd and S. Sastry, Adaptive control: stability, convergence, and robustness, Prentice Hall, USA, 1989.

[20] G. C. Goodwin and D. Q. Mayne, A parameter estimation perspective of continuous time model reference adaptive control, *Automatica (Journal of IFAC)*, Vol. 232, pp. 57-70, 1987.